



PERFORMANCE STUDY OF DSTATCOM WITH PI CONTROLLED SVPWM AND HYSTERESIS CURRENT CONTROLLER FOR POWER FACTOR IMPROVEMENT

K. Murugesan, D. Sai Praveen, Tathagata Mitra and Ranganath Muthu

Department of EEE, SSN College of Engineering, Kalavakkam-603110 (near Chennai), Tamil Nadu, India

E-Mail: murugesank@ssn.edu.in

ABSTRACT

A Distribution STATCOM (DSTATCOM) is a current controlled Voltage Source Converter (VSC) used for reactive power compensation, when connected to the power system. The DSTATCOM using PI controlled Space Vector Pulse Width Modulation (SVPWM) technique has high peak overshoot and large settling time. SVPWM technique requires Phase Locked Loop (PLL) for measurement of varying frequency that is required for Park's transformation and for control. This paper presents a DSTATCOM for reactive power compensation using space vector based Hysteresis Current Controller (HCC) and compares its performance with that of the PI controlled SVPWM method. The HCC technique is robust and has faster transient performance compared to SVPWM control technique. In addition, this technique does not require PLL for measurement of frequency, has reduced switching losses, and is easy to implement. The performance of DSTATCOM with HCC is studied in MATLAB/SIMULINK environment.

Keywords: current controller, DSTATCOM, hysteresis current controller, voltage source converter, SVPWM, PLL.

1. INTRODUCTION

Maintaining power quality in a power system is very essential in today's scenario because of the increase in wide variety of loads that pollute the power system. Inductive loads like induction generators, induction motors, power transformers and arc furnaces, require reactive power for their magnetization and if the reactive power is consumed from the grid, a voltage dip occurs. This voltage dip affects other sensitive loads that are connected to the grid. Hence, it is necessary for inductive load users to compensate for the required reactive power. If the reactive power supplied by the compensator is more than the requirement of the grid, voltage swell occurs, which again affects sensitive loads. Various compensation schemes such as series compensation and shunt compensation have been proposed in the literature [1-2]. Fixed capacitor can supply a fixed amount of reactive power but fails for dynamic loads. Static VAR compensator can generate or absorb the required reactive power by connecting and disconnecting capacitor banks and reactor banks to the network by proper switching action, but has poor transient response and poor dynamic performance.

A DSTATCOM is a shunt compensation device that provides an effective solution for reactive power compensation and voltage regulation. It consists of a Voltage Source Converter (VSC), a DC capacitor, a coupling inductor or coupling transformer and a controller. The DSTATCOM, connected to the grid through a coupling inductor at the Point of Common Coupling (PCC), is controlled in such a way that it exchanges only reactive power with the grid. This is achieved by injecting the current in quadrature with the grid voltage. If the magnitude of DSTATCOM voltage (V_C) is greater than the grid voltage (V_S), the DSTATCOM supplies reactive power to the grid as shown in Figure-1 (a) and the DSTATCOM is operating in the capacitive mode. If the grid voltage (V_S) is greater than the DSTATCOM voltage (V_C), the DSTATCOM absorbs reactive power from the grid as shown in Figure-1(b), and is operating in the inductive mode. If the grid voltage and DSTATCOM voltage are of the same magnitude, there is no exchange of reactive power between the grid and DSTATCOM, as shown in Figure-1(c) and the DSTATCOM is said to be in the floating state. The proposed HCC method has many advantages such as being robust, having very fast response time and being independent of load dynamics.

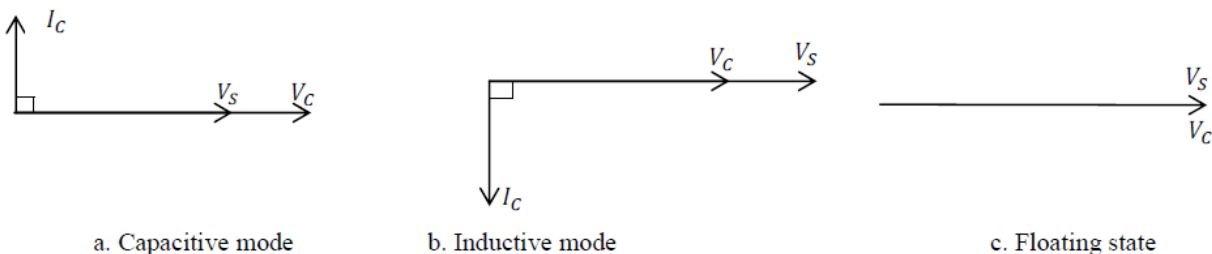


Figure-1. DSTATCOM operating modes.



2. CONTROL STRATEGY FOR DYNAMIC LOADS

Figure-2 shows the single line diagram of a grid connected DSTATCOM at the Point of Common Coupling (PCC) through the coupling inductor or filter. The DSTATCOM consists of a two level VSC, DC capacitor

and a control circuit. Loads connected to the grid can vary dynamically, which is also shown in the figure. The reactive power required by the load is supplied by DSTATCOM by appropriate control action.

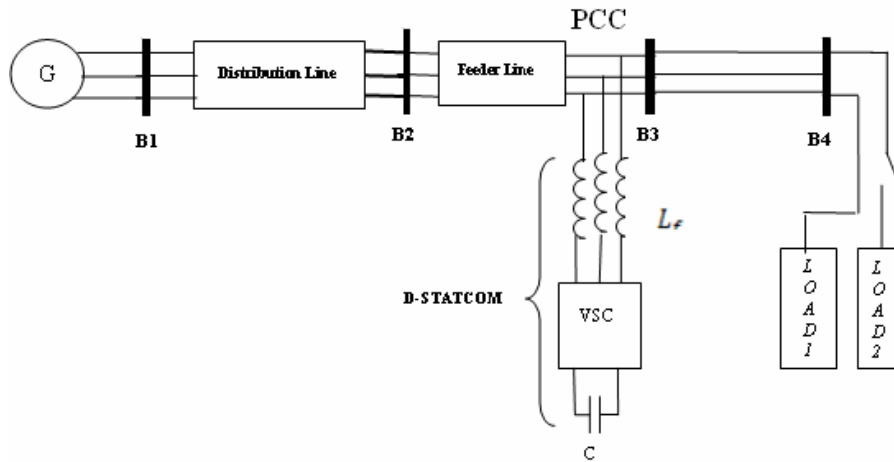


Figure-2. Single line diagram of a DSTATCOM with dynamic loads.

The aim of the proposed SVM-HCC based DSTATCOM is to supply the required reactive power to the load resulting in improvement of power factor. SVM-HCC is a current control technique that requires a reference for its control. The reference current is computed from the instantaneous active power (p) and instantaneous reactive power (q) equations of the load in $\alpha\beta$ frame [3-5], as given by Equation (1).

$$\begin{bmatrix} p \\ q \end{bmatrix} = \begin{bmatrix} v_\alpha & v_\beta \\ -v_\beta & v_\alpha \end{bmatrix} \begin{bmatrix} i_\alpha \\ i_\beta \end{bmatrix} \quad (1)$$

Where

$v_\alpha, v_\beta, i_\alpha, i_\beta$ - are stationary α - β frame representation of 3-phase voltages and currents.

The reference current required for the HCC can be evaluated from the instantaneous values of active power (p^*) and reactive power (q^*) to be supplied by the DSTATCOM, using expressions given in Equations (2) and (3).

$$\begin{bmatrix} i_\alpha^* \\ i_\beta^* \end{bmatrix} = \begin{bmatrix} v_\alpha & v_\beta \\ -v_\beta & v_\alpha \end{bmatrix}^{-1} \begin{bmatrix} p^* \\ q^* \end{bmatrix} \quad (2)$$

$$\begin{bmatrix} i_\alpha^* \\ i_\beta^* \end{bmatrix} = \frac{1}{v_\alpha^2 + v_\beta^2} \begin{bmatrix} v_\alpha & -v_\beta \\ v_\beta & v_\alpha \end{bmatrix} \begin{bmatrix} p^* \\ q^* \end{bmatrix} \quad (3)$$

The instantaneous active power (p^*) that is to be supplied by the DSTATCOM can be evaluated from the energy stored in the DC capacitor and is given by:

$$p^* = -\frac{dE}{dt} = \frac{1}{2}C \frac{d(V_{DC}^2)}{dt} \quad (4)$$

where, V_{DC} is the capacitor voltage.

To improve the power factor, only reactive power is to be compensated and the steady state value of p^* should be zero, which is ensured by maintaining a constant capacitor voltage. The instantaneous reactive power to be compensated (q^*) must be equal and opposite to that of the instantaneous load reactive power requirement ($-q_L$). Hence, Equation (3) is modified and it gives Equation (5).

$$\begin{bmatrix} i_\alpha^* \\ i_\beta^* \end{bmatrix} = \frac{1}{v_\alpha^2 + v_\beta^2} \begin{bmatrix} v_\alpha & -v_\beta \\ v_\beta & v_\alpha \end{bmatrix} \begin{bmatrix} 0 \\ -q_L \end{bmatrix} \quad (5)$$

Equation (5) gives the reference current in $\alpha\beta$ frame, which is to be compared with the actual current of the DSTATCOM in the same frame of reference, and fed to the HCC as shown in Figure-3.

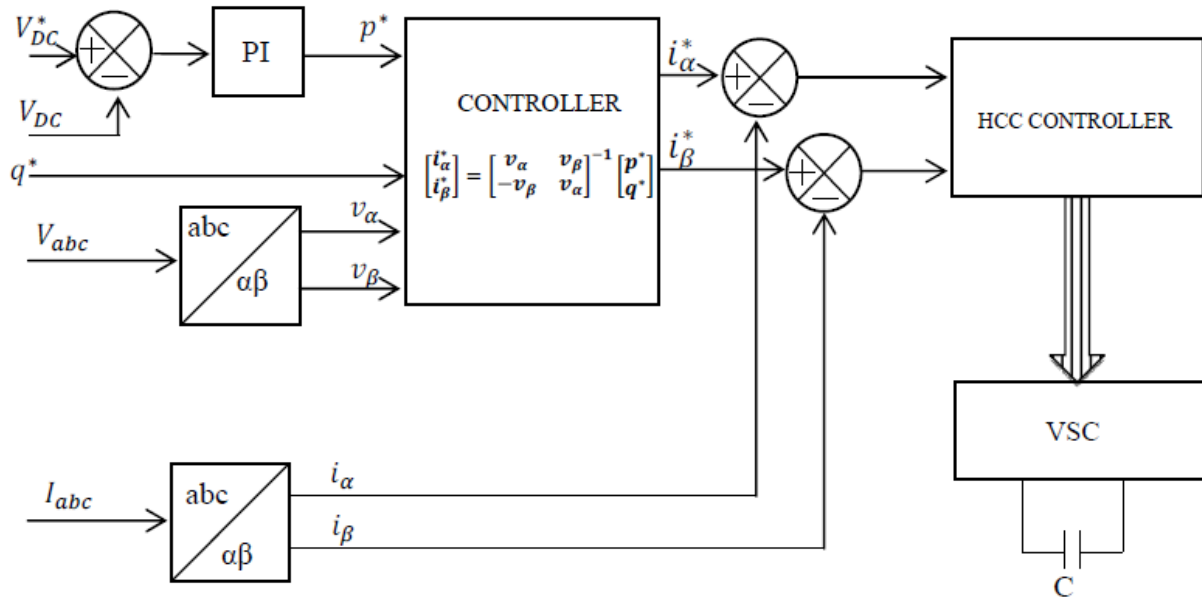


Figure-3. Block diagram of SVM based HCC.

3. PRINCIPLE OF HYSTERESIS CURRENT CONTROLLER

Hysteresis current control is an instantaneous closed loop control technique in which the output current i of the inverter is made to track the command current i^* and maintain the error within the hysteresis band (δ). When the error in current ($i_e = i^* - i$) crosses the error band, inverters are switched to bring the output current within the error band as shown in Figure-4. When the output current exceeds the upper band ($i^* + \delta/2$), it is brought back to within the band of δ by turning ON the lower switch and turning OFF the upper switch of the inverter leg of the phase considered. As a result, the voltage across the load changes from V_{DC} to 0 and the current decreases. Similarly when the output current goes below the lower

band ($i^* - \delta/2$), the load is connected to V_{DC} by turning

OFF the lower switch and turning ON the upper switch. As a result, the output voltage across the load changes from 0 to V_{DC} and the output current starts to build up. An optimal value of δ must be chosen to maintain a balance between the output current ripple and the switching losses and thereby eliminate particular harmonics [5-9]. In this

control technique, since each phase is controlled independently, switching frequency goes abnormally high, which increases the switching losses. In this paper, a vector based control technique is proposed, which decreases the slope of the error in current by controlling the switching frequency.

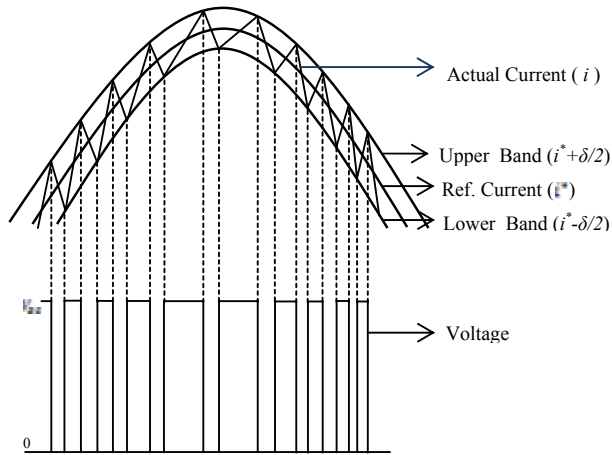


Figure-4. Hysteresis band.

4. SPACE VECTOR BASED CONTROL

In space vector modulation technique, three phase quantities are transformed to their equivalent two phase quantities, in the stationary reference frame. From these two-phase components, the magnitude of reference vector is computed, which is used for modulating the inverter output [10-12].

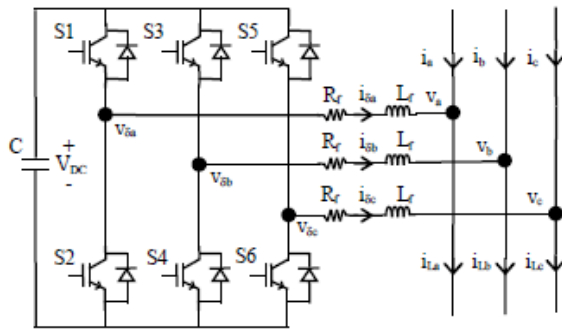


Figure-5. STATCOM Configuration.

The state space representation of VSC based DSTATCOM is obtained by applying Kirchoff's voltage law to Figure-5.

$$\frac{di_{\delta a}}{dt} = \frac{1}{3L_f} [2(v_{\delta a} - v_a) - (v_{\delta b} - v_b) - (v_{\delta c} - v_c)] - \frac{R_f}{L_f} i_{\delta a} \quad (6)$$

$$\frac{di_{\delta b}}{dt} = \frac{1}{3L_f} [2(v_{\delta b} - v_b) - (v_{\delta c} - v_c) - (v_{\delta a} - v_a)] - \frac{R_f}{L_f} i_{\delta b} \quad (7)$$

$$\frac{di_{\delta c}}{dt} = \frac{1}{3L_f} [2(v_{\delta c} - v_c) - (v_{\delta a} - v_a) - (v_{\delta b} - v_b)] - \frac{R_f}{L_f} i_{\delta c} \quad (8)$$

where, $i_{\delta abc}$ are the DSTATCOM output currents, $v_{\delta abc}$ are the DSTATCOM phase voltages and v_{abc} are the grid phase voltages.

Equations (6) to (8) can be written in vector form using Clark's transformation, as given in Equation (9).

$$\frac{di_0}{dt} = \frac{1}{L} (V_n - v_0) - \frac{R}{L} i_0 \quad (9)$$

where, i_0 is the VSC output current vector, V_n is the VSC output voltage vector and v_0 is the grid voltage vector.

Defining i^* as the reference current vector and i_e as the error in current vector, we get

$$i_e = i^* - i_0 \quad (10)$$

From Equations (9) and (10), differential equations describing the error in current vector are derived as:

$$\frac{di_e}{dt} = \frac{di^*}{dt} - \frac{di_0}{dt}$$

$$L_f \frac{di_e}{dt} + R_f i_e = L_f \frac{di^*}{dt} + R i^* - (V_n - v_0) \quad (11)$$

It is observed from Equation (11) that the error in current vector (i_e) varies with time constant (L/R) and is influenced by the reference current vector and its derivative (i^* and $\frac{di^*}{dt}$), as well as the inverter output voltage vector (V_n) and the grid voltage vector (v_0). Neglecting R in Equation (11), the desired inverter output voltage to achieve zero error can be defined by:

$$V_n^* = v_0 + L_f \frac{di^*}{dt} \quad (12)$$

$$L_f \frac{di_e}{dt} = V_n^* - V_n \quad (13)$$

It can be seen that the information of the grid voltage vector and the derivative of the reference current vector are required to nullify the inverter tracking error.

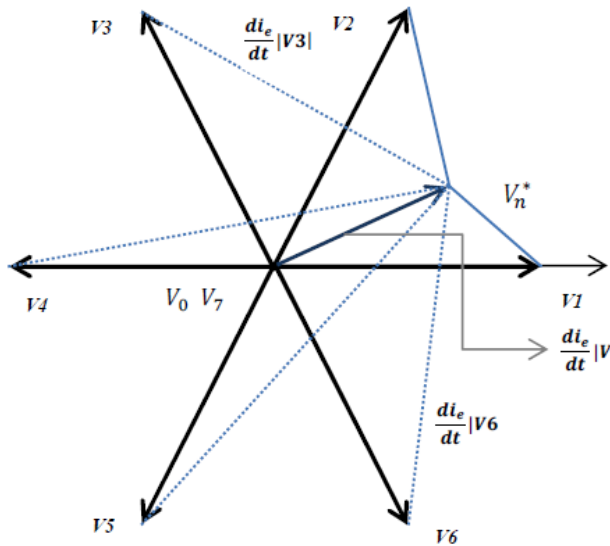


Figure-6. Derivatives of error in current vector when V_n^* is in Sector I.

Space Vector based hysteresis control method is used, in which the desired reference voltage (V_n^*) in each sector is found by choosing two adjacent non-zero vectors and a zero vector. For example, let the desired output voltage vector (V_n^*) be located in Sector I, as shown in

Figure-6. To follow the reference voltage vector, $\frac{di_e}{dt}$ needs to be very small. This condition is satisfied if the voltage vectors adjacent to reference voltage vector (V_n^*) are selected (e.g. V_1, V_2, V_0 and V_7 for Sector I). In this way, two adjacent non-zero voltage vectors and a zero voltage vector (v_0) are selected by the controller to reduce the tracking error. Accordingly, the proposed vector-based current controller generates a switching pattern similar to the well-known Space Vector Modulation (SVM) under steady-state conditions. It should be noted that to produce this optimal switching pattern, only the sector of V_n^* needs to be determined and not the exact value of the vector. During transient conditions, non-optimal voltage vectors with high value of derivative of error in current must be applied to force the error vector into the hysteresis band as fast as possible. This would provide a very fast transient response for the vector-based current controller.

5. SPACE VECTOR BASED HYSTERESIS CURRENT CONTROL METHOD

In this paper, SVM based HCC is implemented with multilevel hysteresis comparators for controlling output current of the DSTATCOM. The error in current is

represented in stationary (α - β) frame and the error in current vector is controlled to lie within the tolerance region [13-15]. Figure-7 shows the VSC output voltage space vectors in α - β plane. Table-1 gives the possible switching states and corresponding normalized α - β values of vectors. It can be observed that there are three discrete levels along β axis and four discrete levels along α axis. Hence, to identify the region of the error in the current vector, a four-level hysteresis comparator on α axis and a three-level hysteresis comparator on β axis are used. A new voltage vector with the opposite value of α (or β) component is applied when the DSTATCOM output current exceeds the tolerance region on one particular axis. Suppose the DSTATCOM output current is in sector I, and if error exceeds the tolerance region from the bottom (or top) side, the next voltage vector with larger (or smaller) value of β component is applied to bring the error in the current vector within the tolerance region. Similarly, if the output current exceeds the tolerance region from the left (or right) side, the next voltage vector with larger value (or smaller) of α component is applied to bring the error in current vector inside the tolerance region. For all other cases, the current controller must select zero voltage vectors to achieve minimum switching losses.

The DSTATCOM output voltage in stationary reference frame can have four values of non-zero voltage vectors in α axis and three values of non-zero voltage vectors in β axis, as shown in Figure-7. Therefore, a current controller of four level comparators in α axis and three-level comparators in β axes is used in this method. The outputs of hysteresis comparators $D\alpha$ (in α axis) and $D\beta$ (in β axis) determine the output voltage vector of the DSTATCOM, as shown in Figure-7 and tabulated in Table-2. These vectors are chosen in such a way that the slope of the error in current vector and error is within the square tolerance region. For each 60° , the comparator outputs, $D\alpha$ and $D\beta$, remain constant from which the sector information of reference voltage vector V_n^* is obtained. Hence, the controller should select two non-zero voltage vectors adjacent to the reference voltage vector V_n^* and a zero voltage vector. Once the value of $D\alpha$ or $D\beta$ changes, the reference voltage vector V_n^* moves to the next sector. In each sector, the controller selects two non-zero voltage vectors and a zero vector, as done in the previous sector. Thus, by this method, the switching frequency of the inverter is significantly reduced.

Table-1. Three-phase switching states, respective voltage space vectors and their - β values.



S_a^*	S_b^*	S_c^*	V_n	$\frac{V_\alpha}{V_{dc}}$	$\frac{V_\beta}{V_{dc}}$
0	0	0	V_0^0	0	0
1	0	0	V_1	2/3	0
1	1	0	V_2	1/3	$1/\sqrt{3}$
0	1	0	V_3	-1/3	$1/\sqrt{3}$
0	1	1	V_4	-2/3	0
0	0	1	V_5	-1/3	$-1/\sqrt{3}$
1	0	1	V_6	1/3	$-1/\sqrt{3}$
1	1	1	V_0^1	0	0

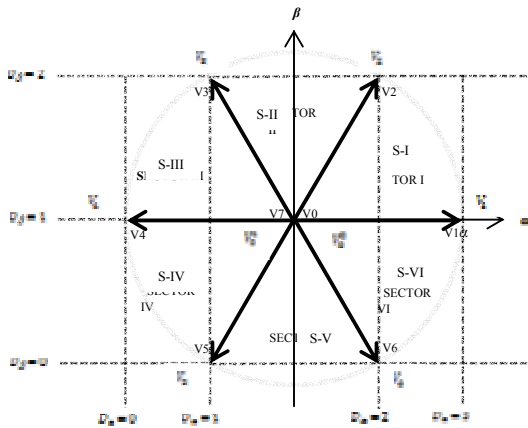


Figure-7. Determining sector information from Hysteresis Comparator outputs.

Table-2. Switching table of the proposed vector-based HCC method.

$D\beta$ / $D\alpha$	0	1	2
0	V_5	V_4	V_3
1	V_5	V_0	V_3
2	V_6	V_0	V_2
3	V_6	V_1	V_2

6. SIMULATION

Simulation studies are carried out to verify the validity of the Hysteresis Current Controller (HCC) and compare its performance with PI controlled Space Vector PWM method. A grid connected DSTATCOM is simulated for dynamic load variation to compensate for

the reactive power and to improve the power factor of the system. The entire system is simulated in MATLAB/Simulink with parameters given in Appendix I.

The simulation results for HCC are shown in Figures 8 - 15. For simulation from time $t = 0$ to $t = 0.1s$, only load1 is connected to the system and at $t = 0.1s$, load2 is connected to the system, in addition to load1. It is noted that from Figure-8 that the load current at $t = 0.1s$ increases sharply from 0.3 pu to 0.6 pu without any transient delay. The additional load needs more load current and the same is supplied immediately in HCC method. Figures 9-10 respectively show source voltage and current variations and load voltage and current variations. It can be inferred from these results that the source voltage and current are in phase for all conditions. Hence, on load side, the HCC reduces the angle between voltage and current by injecting appropriate reactive power from DSTATCOM (i.e., $Q = 0.2$ pu to 0.4 pu) as shown in Figure-15, thus improving the load power factor. The supplied reactive power also maintains grid voltage constantly at 1 pu as shown in Figure-11. During the load variation, DSTATCOM is controlled in such a way that it does not supply any active power to the system as shown in Figure-14, and this is ensured by keeping the capacitor voltage constant (V_c) at 1120V. It is also achieved by HCC as shown in Figure-12.

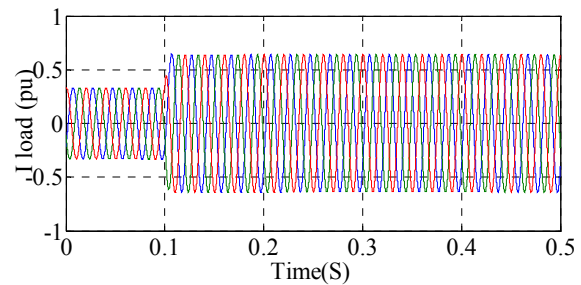


Figure-8. Load current variation.

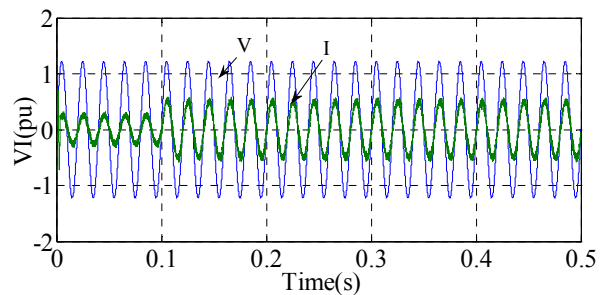


Figure-9. Source voltage and current.

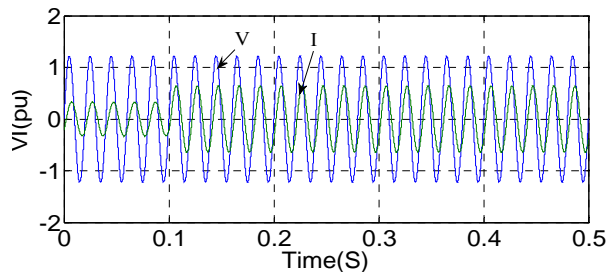


Figure-10. Load voltage and current.

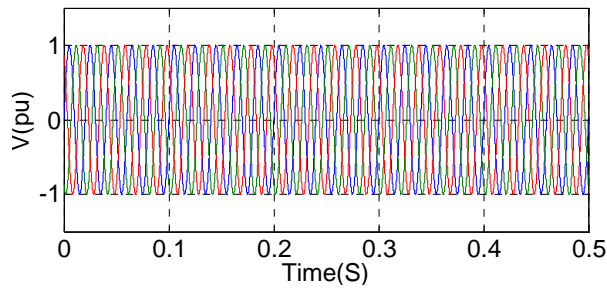


Figure-11. Grid voltage.

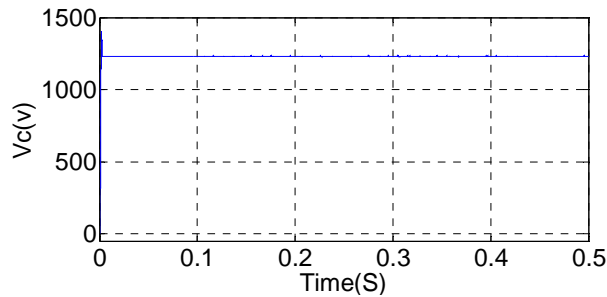


Figure-12. DC capacitor voltage.

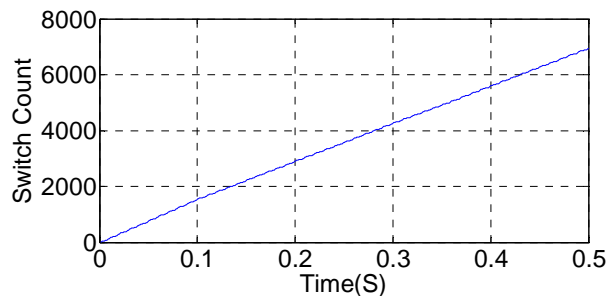


Figure-13. Switch count.

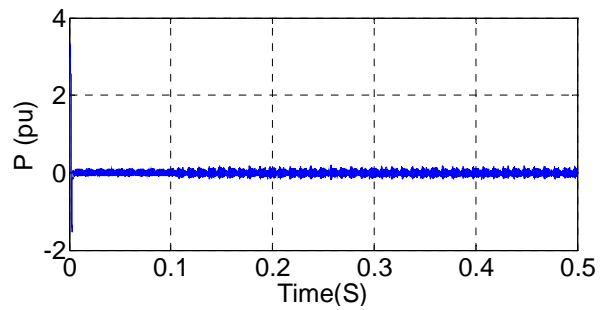


Figure-14. Real power supplied by D-STATCOM.

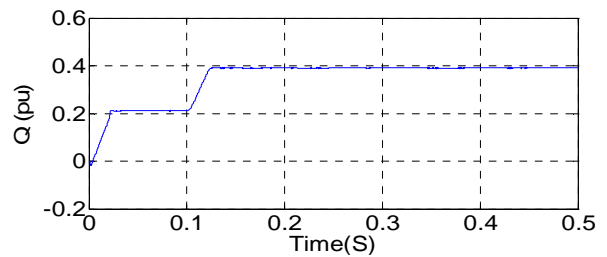


Figure-15. Reactive power supplied by DSTATCOM.

For the same situation, when the DSTATCOM is controlled using PI controller with SVPWM algorithm, the simulation results are shown in Figures 16 -18. It is found that the DC capacitor voltage, active power and reactive power controllers have large transient responses whereas the HCC, a robust controller, does not have any transient delay, with reduced switching losses.

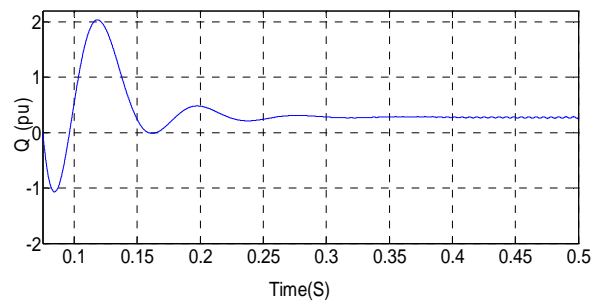


Figure-16. Reactive power supplied by DSTATCOM.

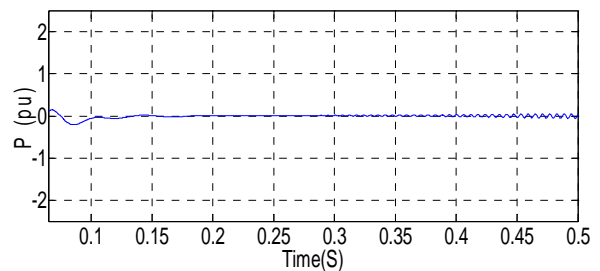


Figure-17. Active power supplied by DSTATCOM.

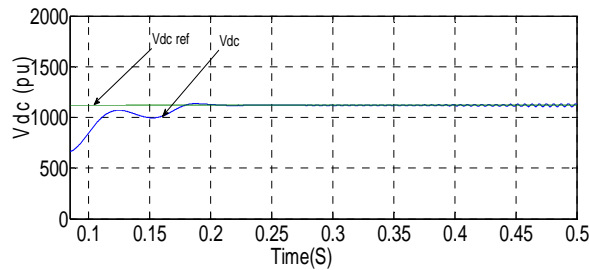


Figure-18. Capacitor voltage.

7. CONCLUSIONS

This paper presents a comparative performance study of a DSTATCOM for power factor improvement using PI controlled SVPWM method and SVM based HCC method. It is found that both controllers were able to achieve their control objectives, but PI controlled SVPWM method had larger transient time compared to SVM based HCC method. HCC method is found to achieve steady state values faster, which is essential for a good controller. It can be concluded that the SVM based HCC performs better for dynamic loads. It should also be noted that the SVM based HCC has faster transient response with minimum switching losses compared to PI controlled SVPWM method.

Appendix-I

Base Voltage (V)	400
Base kVA (VA)	28
Line Resistance (Ohms)	2
Line Inductance (mH)	1
VSC Filter Inductance (mH)	10
Load A (Ohms)	$5 + j7.85$
Load B (Ohms)	$10 + j3.14$
Capacitance of DC Capacitor (μC)	330
DC Capacitor Reference Voltage (V)	1120
Three level Hysteresis Comparator	
δ_1 (A)	0.06
δ_2 (A)	0.04
δ_3 (A)	0.02
Four level Hysteresis Comparator	
δ_1 (A)	0.04
δ_2 (A)	0.02
Sampling Frequency (kHz)	5

ACKNOWLEDGEMENT

We sincerely express our thanks to SSN Educational Trust for their encouragement and financial support to carry out this project.

REFERENCES

- [1] Hingorani N.G. and L. Gyugyi. 2000. Understanding FACTS: Concepts and Technology of Flexible AC Transmission Systems. New York: IEEE Press. pp. 135-143.
- [2] Bose B.K. 2002. Power Electronics and Electrical AC Drives. Prentice-Hall.
- [3] Akagi Hirofumi, Kanazawa Yoshihira and Nabae Akira. 1984. Instantaneous Reactive Power Compensators Comprising Switching Devices without Energy Storage Components. IEEE Transactions on Industry Applications. IA- 20(3): 625-630, May.
- [4] Ching-Tsai Pan and Ting-Yu Chang. 1994. An improved hysteresis current controller for reducing switching frequency. IEEE Transactions on Power Electronics. 9(1): 97-104, Jan.
- [5] Fang Zheng Peng and Jih-Sheng Lai. 1996. Generalized instantaneous reactive power theory for three-phase power systems. IEEE Transactions on Instrumentation and Measurement. 45(1): 293-297, Feb.
- [6] Bong-Hwan Kwon, Tae-Woo Kim and Jang-Hyoun Youm. 1998. A novel SVM-based hysteresis current controller. IEEE Transactions on Power Electronics. 13(2): 297-307, Mar.
- [7] Mohapatra M. and Babu B.C. 2010. Fixed and sinusoidal-band hysteresis current controller for PWM voltage source inverter with LC filter. Proceedings of 2010 IEEE Students' Technology Symposium (TechSym). pp. 88-93, 3-4 April.
- [8] Malesani L. and Tenti P. 1990. A novel hysteresis control method for current-controlled voltage-source PWM inverters with constant modulation frequency. IEEE Transactions on Industry Applications. 26(1): 88-92, Jan/Feb.
- [9] Tahri F., Tahri A., AlRadadi A. and Draou A. 2007. Analysis and control of advanced static VAR compensator based on the theory of the instantaneous reactive power. Proceedings of International Aegean Conference on Electrical Machines and Power Electronics. ACEMP '07, pp. 840-845, 10-12 Sept.
- [10] Kazmierkowski M.P. and Malesani L. 1998. Current control techniques for three-phase voltage-source PWM converters: a survey. IEEE Transactions on Industrial Electronics. 45(5): 691-703, Oct.
- [11] D. W. Novotny and T. A. Lipo. 1996. Vector Control and Dynamics of AC Drives. Oxford, U.K. Clarendon.
- [12] C. T. Pan and T. Y. Chang. 1994. An improved hysteresis current controller for reducing switching frequency. IEEE Trans. on Power Electron. 9: 97-104, Jan.
- [13] Mohseni M. and Islam S.M. 2010. A New Vector-Based Hysteresis Current Control Scheme for Three-



www.arpnjournals.com

Phase PWM Voltage-Source Inverters. IEEE Transactions on Power Electronics. 25(9): 2299-2309, Sept.

- [14]Tilli A. and Tonielli A. 1998. Sequential design of hysteresis current controller for three-phase inverter. IEEE Transactions on Industrial Electronics. 45(5): 771-781, Oct.
- [15]Bong-Hwan Kwon, Tae-Woo Kim and Jang-Hyoun Youm. 1998. A novel SVM-based hysteresis current controller. IEEE Transactions on Power Electronics. 13(2): 297-307, Mar.